various domains, including wind energy, smart home automation, and digital power grids. These models enable real-time processing of data, reduce processing time, and improve the accuracy of results.

Wireless offloading has become an increasingly popular approach for reducing the processing load of mobile devices by offloading computation tasks to more powerful remote servers [20–22]. Several studies have explored the use of wireless offloading in various domains, including image processing, machine learning, and mobile health. One study devised a wireless offloading scheme for image recognition tasks in mobile devices, where a multi-access edge computing (MEC) architecture was utilized to offload computation tasks to nearby servers, resulting in reduced energy consumption and improved processing speed. Another study investigated the use of wireless offloading for machine learning tasks in mobile devices [23–27].This study investigated a federated learning framework that utilized wireless offloading to distribute computation tasks to remote servers. The investigated framework was shown to be effective in reducing the processing load of mobile devices while maintaining high accuracy.

In the context of wireless networks, several studies have explored the impact of wireless offloading on network outage probability. One study investigated the impact of wireless offloading on the outage probability of multi-hop wireless networks. This study demonstrated that the use of wireless offloading could reduce the outage probability of multi-hop wireless networks. Another study devised a wireless offloading scheme for device-to-device (D2D) communication in cellular networks, where a social network-based approach was utilized to offload data transmission tasks to nearby devices. This study demonstrated that the devised scheme was effective in reducing the outage probability of D2D communication in cellular networks. In a word, wireless offloading has shown great promise in reducing the processing load of mobile devices and improving the performance of wireless networks. Several studies have explored the use of wireless offloading in various domains and have shown its effectiveness in reducing energy consumption, improving processing speed, and reducing network outage probability.

Motivated by the above literature review, this paper presents a real-time distributed computing model that deals with low-voltage flow data in digital power grids operating in autonomous and controllable environments. The proposed model uses edge computing through wireless offloading to process and analyze the data generated by low-voltage devices more efficiently. Firstly, we evaluate the performance of the system under consideration by measuring its outage probability, utilizing both the received signal-to-noise ratio (SNR) and communication and computing latency.

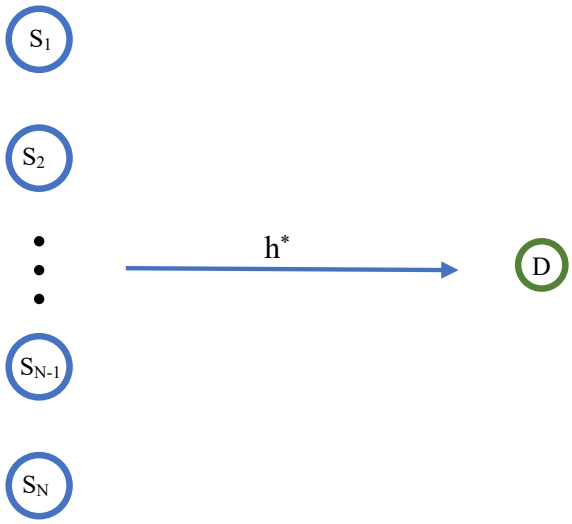

Figure 1. System model of real-time distributed computing.

Subsequently, we analyze the system outage probability by deriving an analytical expression. To this end, we utilize the Gauss-Chebyshev approximation to provide an approximate closed-form expression. Experimental evaluations indicate that the proposed model effectively achieves real-time processing of low-voltage flow data in digital power grids. This model offers an effective and practical solution for handling low-voltage flow data, making it a valuable addition to the digital power grids domain.

2. System Model

The system under consideration, as shown in Figure 1, is a task offloading system that comprises multiple source nodes $S_n|1 \leq n \leq N$ and a single CAP node. Each source node S_n in this system is furnished with a single antenna, and the wireless communication between them and the CAP node takes place via a wireless channel. Due to the limited computing capacity of source nodes, it is difficult to complete computing tasks within a fixed time frame. Therefore, task offloading to the CAP node is necessary to accelerate the computing process. Additionally, due to various factors such as the differing properties of tasks in source nodes, the task size l may vary in practice. Assuming a uniform distribution of task size within the interval $l \in [L_{min}, L_{max}]$, without loss of generality. Considering that both the source nodes and the CAP node are equipped with only one antenna, it is reasonable to assume that the links within the network experience Rayleigh fading.

2.1. Transmission Model

When the source node S_n needs to offload tasks to the CAP node, in order to ensure the stability of data transmission and reduce transmission delay, the source node S_n with the optimal channel should be selected for task offloading as,

$$|h_*|^2 = \max\{|h_1^2, ..., |h_n|^2, ..., |h_N|^2\}, \tag{1}$$

where $h_n \sim \mathcal{CN}(0, \beta)$ is the instantaneous channel parameter from the source node S_n to D. The CAP node's received SNR is expressed as,

$$SNR^* = \frac{P}{\sigma^2}|h_*|^2, \tag{2}$$

where the variance of AWGN at the CAP is σ^2, and the transmit power at the source node S_n is P. The rate of transmission is,

$$R^* = B\log_2(1 + SNR^*), \tag{3}$$

The transmission delay is determined by the wireless transmission bandwidth, which is denoted as B,

$$T_c = \frac{l}{R^*}. \tag{4}$$

2.2. Computation Model

The calculation latency after task offloading from the source node S_n to the CAP is shown below,

$$T_f = \frac{l}{f_d}, \tag{5}$$

where f_d represents the computational capability available at the CAP. The total delay of the system is,

$$T = T_c + T_f. \tag{6}$$

3. Outage probability analysis

In practice, each source node has different sizes of computation tasks and experiences different fading channels, resulting in different times for task transmission and computation. However, there are fixed threshold limits for different tasks, which must be completed within a specified time. Specifically, when the total delay is larger than the delay threshold, the system is considered to be interrupted, and the interruption probability can be expressed as,

$$P_{out} = \Pr\{T < Y_t\}. \tag{7}$$

In further, (7) can be expanded as,

$$P_{out} = \Pr\left\{\frac{l}{B\log_2(1 + \frac{P}{\sigma^2}|h_*|^2)} + \frac{l}{f_d} < Y_t\right\}. \tag{8}$$

We can transform (8) to obtain,

$$P_{out} = \Pr\left\{\frac{l}{B\log_2(1 + \frac{P}{\sigma^2}|h_*|^2)} + \frac{l}{f_d} < Y_t\right\}, \tag{9}$$

$$= \Pr\left\{\frac{l}{\log_2(1 + \frac{P}{\sigma^2}|h_*|^2)} < Y_t - \frac{l}{f_d}\right\}. \tag{10}$$

We can rewrite (10) as

$$P_{out} = \Pr\left\{|h_*|^2 < \left(2^{\frac{l}{Y_t - \frac{l}{f_d}}} - 1\right)\frac{\sigma^2}{P}\right\}. \tag{11}$$

From (1), we can write the cumulative density function of $|h_*|^2$ as,

$$F_{|h_*|^2}(y) = (1 - e^{-\frac{y}{\beta}})^N, \tag{12}$$

$$= \sum_{n=0}^{N}\binom{N}{n}(-1)^n e^{-\frac{ny}{\beta}}. \tag{13}$$

Accordingly, we can rewrite the conditional outage probability $P_{out}(Y_t|l)$ with respect to the task size l as [28],

$$P_{out}(Y_t|l) = \int_0^{G(x)} f_{|h_*|^2}(y)dy, \tag{14}$$

with

$$G(l) = \left(2^{\frac{x}{Y_t - \frac{l}{f_d}}} - 1\right)\frac{\sigma^2}{P}. \tag{15}$$

From (13), we can derive the conditional outage probability $P_{out}(Y_t|l)$ as,

$$P_{out}(Y_t|l) = \sum_{n=0}^{N}\binom{N}{n}(-1)^n e^{-\frac{nG(l)}{\beta}}. \tag{16}$$

From $P_{out}(Y_t|l)$ and $l \sim \mathcal{U}[L_{min}, L_{max}]$, we can further derive P_{out} as,

$$P_{out} = \int_{L_{min}}^{L_{max}} \frac{P_{out}(Y_t|l)}{L_{max} - L_{min}}dl, \tag{17}$$

$$= \sum_{n=0}^{N}\binom{N}{n}\frac{(-1)^n)}{L_{max} - L_{min}}\int_{L_{min}}^{L_{max}} e^{-\frac{nG(l)}{\beta}}dl. \tag{18}$$

As it is difficult to obtain an exact solution for the abvoe P_{out}, we turn to find an approximate result. We use the Gauss-Chebyshev quadrature method to approximate the result, which is a widely-used integration method that has proven to be effective. Specifically, the approximate P_{out} can be rewritten as,

$$P_{out} = \sum_{n=0}^{N}\sum_{k=0}^{K}\binom{N}{n}\frac{(-1)^n)}{L_{max} - L_{min}}w_k e^{-\frac{nG(w_k)}{\beta}}, \tag{19}$$

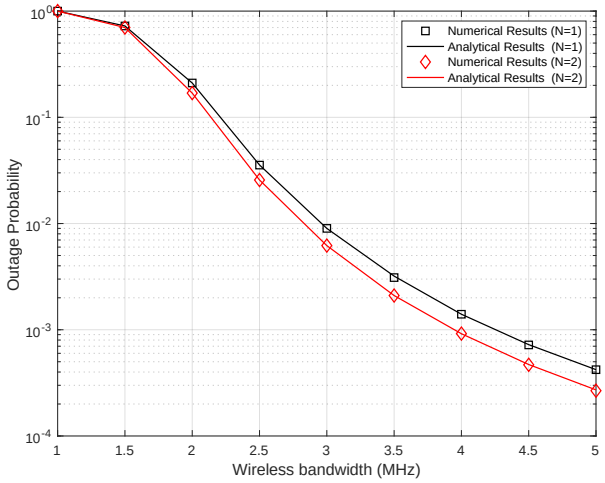

Figure 2. Outage probability versus the wireless bandwidth.

where K denotes the number of truncated terms in the Gauss-Chebyshev quadrature approximation, and w_k is

$$w_k = \frac{(L_{max} - L_{min})\pi}{2K} \sin(z_k), \tag{20}$$

with

$$z_k = \frac{(2k+1)\pi}{2K}. \tag{21}$$

In particular, a larger K leads to a more accurate approximation in calculating P_{out}, while a smaller K will deteriorate the approximation performance with the benefit of reduced computational complexity in the approximation.

4. NUMERICAL AND SIMULATION RESULTS

In this section, we compared the numerical and analytical results of the system outage probability for different numbers of source nodes. Unless specified, the simulation environment is configured as follows. The task of source nodes is uniformly distributed in the range of [5,10] Mb, the transmit power is $P = 3$ W, and the latency threshold is $Y_t = 8$. Additionally, $F = 5 \times 10^8$ cycles per second is set.

The effect of wireless bandwidths on the system outage probability is shown in Figure 2 and Table 1. The number of source nodes S_n varies from 1 to 2, the wireless bandwidth ranges from 1 MHz to 5 MHz, and the transmit power is set to 2 W. The results demonstrate the accuracy of the analytical results for different numbers of source nodes, as both the numerical and analytical results are nearly identical under different numbers of source nodes, as seen from Figure 2 and Table 1. Additionally, as the bandwidth increases, the outage probability decreases because the additional bandwidth reduces the transmission delay and increases the probability of meeting the latency threshold. Furthermore, involving multiple source nodes in offloading can effectively reduce the outage probability, as evidenced by the decrease in outage probability as the number of source nodes N increases.

The effect of transmit power on the system outage probability is illustrated in Figure 3 and Table 2. The number of source nodes S_n ranges from 1 to 2, the transmit power varies from 1 W to 5 W, and the wireless bandwidth is set to 5 MHz. The results demonstrate the accuracy of the analytical results for different numbers of source nodes, as both the numerical and analytical results are almost identical under different numbers of source nodes, as observed from Figure 3 and Table 2. Additionally, increasing the transmit power reduces the outage probability because it improves the transmission rate, leading to a decrease in the transmission delay and an increase in the probability of meeting the latency thresholds. Moreover, involving multiple source nodes in offloading can effectively decrease the outage probability, as evidenced by the decrease in outage probability with an increase in the number of source nodes N.

Table 3 and Figure 4 illustrate the impact of transmit SNR on the system outage probability. The number of source nodes (S_n) varies from 1 to 2, the transmit SNR ranges from 0 dB to 40 dB, the transmit power is set at 3 W, and the wireless bandwidth is set to 5 MHz. The results demonstrate the accuracy of the analytical results for different numbers of source nodes, as both the numerical and analytical results are nearly identical under different numbers of source nodes, as observed from Figure 4 and Table 3. Additionally, increasing the transmit SNR reduces the outage probability because it improves the transmission

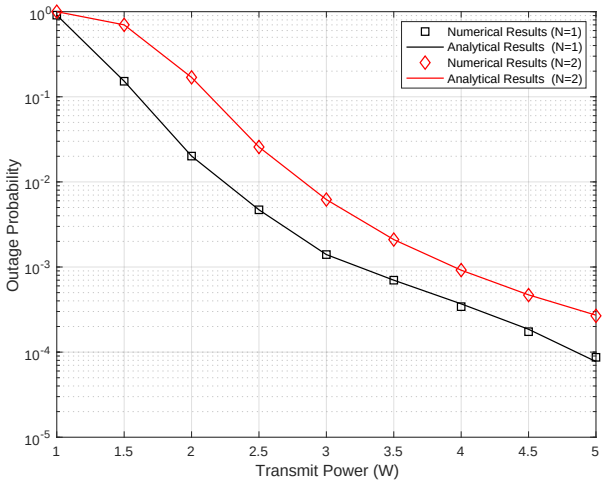

Figure 3. Outage probability versus the transmit power.

Table 1: Numerical outage probability versus the wireless bandwidth.

B(MHz)	1	1.5	2	2.5	3	3.5	4	4.5	5
Numerical (N=1)	1	0.7245	0.2104	0.0356	0.0090	0.0032	0.0014	7.2439e-04	4.2111e-04
Ana. (N=1)	1	0.7245	0.2104	0.0356	0.0090	0.0032	0.0014	7.2439e-04	4.2111e-04
Numerical (N=2)	1	0.7003	0.1691	0.0257	0.0062	0.0021	9.2010e-04	4.6783e-04	2.6683e-04
Ana. (N=2)	1	0.7003	0.1690	0.0257	0.0062	0.0021	9.1774e-04	4.7068e-04	2.7159e-04

Table 2: Numerical outage probability versus the transmit power.

W	1	1.5	2	2.5	3	3.5	4	4.5	5
Numerical (N=1)	0.99	0.2127	0.0301	0.0077	0.0029	0.0014	7.8627e-04	4.9300e-04	3.2833e-04
Ana. (N=1)	0.99	0.2127	0.0301	0.0077	0.0029	0.0014	7.9135e-04	4.9466e-04	3.3374e-04
Numerical (N=2)	0.91	0.1523	0.0201	0.0047	0.0014	0.0007	3.4212e-04	1.7382e-04	0.8691e-04
Ana. (N=2)	0.91	0.1526	0.0201	0.0047	0.0014	0.0007	3.6893e-04	1.8547e-04	0.7741e-04

Table 3: Numerical outage probability versus the transmit SNR.

P/σ^2 (dB)	0	5	10	15	20	25	30
Numerical (N=1)	1	0.0176	0.0039	0.0016	7.9096e-04	4.6611e-04	2.9951e-04
Ana. (N=1)	1	0.0176	0.0039	0.0016	7.9261e-04	4.6524e-04	2.9940e-04
Numerical (N=2)	1	0.0059	8.8923e-04	2.7095e-04	1.1637e-04	5.7911e-05	3.4386e-05
Ana. (N=2)	1	0.0059	8.9134e-04	2.7544e-04	1.1654e-04	5.8984e-05	3.3537e-05

rate, leading to a decrease in the transmission delay and an increase in the probability of meeting the latency threshold. Furthermore, involving multiple source nodes in offloading can effectively decrease the outage probability, as evidenced by the decrease in outage probability with an increase in the number of source nodes N.

Table 4 and Figure 5 illustrate how the computational capability of CAP impacts the system outage probability. The number of source nodes (S_n) varies from 1 to 2, the computational capability of CAP ranges from

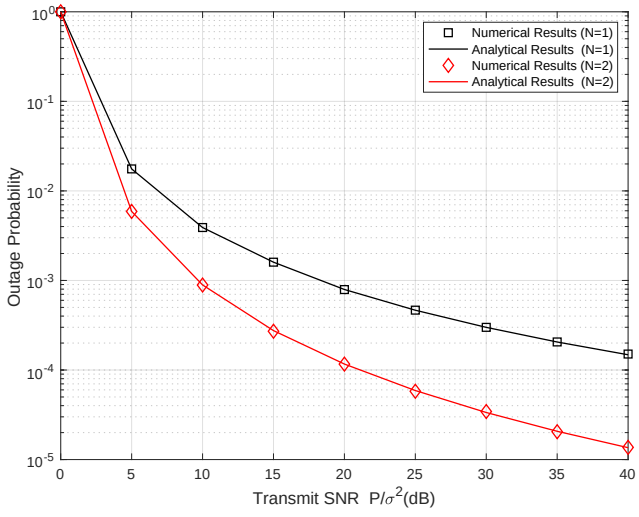

Figure 4. Outage probability versus the transmit SNR.

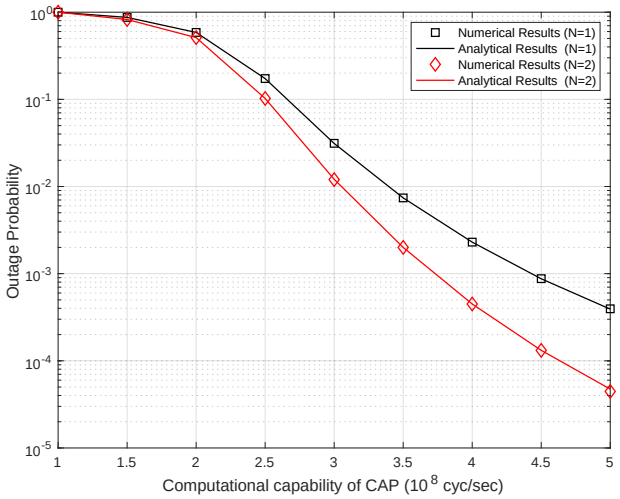

Figure 5. Outage probability versus the computational capability of CAP.

1×10^8 cyc/sec to 5×10^8 cyc/sec, the transmit power is set at 3 W, and the wireless bandwidth is set to 5 MHz. The accuracy of the analytical results for different numbers of source nodes is demonstrated by the close agreement between the numerical and analytical results for different numbers of source nodes, as observed from Figure 5 and Table 4. Increasing the computational capability reduces the outage probability, as a higher f_d reduces the computation time, thereby increasing the

Table 4: Numerical outage probability versus the computational capability of CAP.

$f_d(10^8 cyc/sec)$	1	1.5	2	2.5	3	3.5	4	4.5	5
Numerical (N=1)	1	0.8713	0.5859	0.1732	0.0313	0.0074	0.0023	8.7587e-04	3.9513e-04
Ana. (N=1)	1	0.8716	0.5858	0.1731	0.0312	0.0074	0.0023	8.7336e-04	3.9176e-04
Numerical (N=2)	1	0.8249	0.5114	0.1024	0.0120	0.0020	4.4860e-04	1.3173e-04	4.4533e-05
Ana. (N=2)	1	0.8247	0.5113	0.1024	0.0121	0.0020	4.4846e-04	1.3190e-04	4.7332e-05

Table 5: Numerical outage probability versus the latency threshold.

Latency thresholds (Y_t)	6	7	8	9	10	11	12
Numerical (N=1)	1	0.4989	0.0520	0.0090	0.0026	0.0010	4.8960e-04
Ana. (N=1)	1	0.4990	0.0521	0.0090	0.0026	0.0010	4.8965e-04
Numerical (N=2)	1	0.4361	0.0385	0.0062	0.0017	6.5753e-04	3.1603e-04
Ana. (N=2)	1	0.4360	0.0384	0.0062	0.0017	6.5948e-04	3.1641e-04

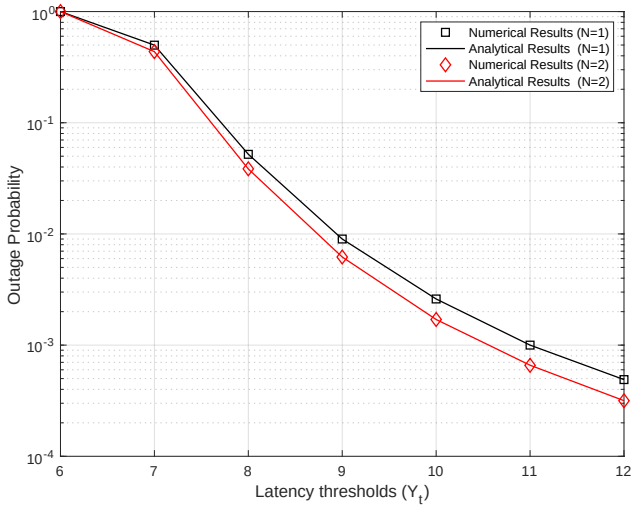

Figure 6. Outage probability versus the latency threshold.

probability of meeting the latency threshold. Furthermore, involving multiple source nodes in offloading can effectively reduce the outage probability, as evidenced by the decrease in outage probability with an increase in the number of source nodes N.

Table 5 and Fig. 6 illustrate the impact of the latency threshold on the system outage probability, where the number of source nodes (S_n) varies from 1 to 2, and the latency threshold varies from 6s to 12s. The transmit power is fixed at 3 W, and the wireless bandwidth is set to 5 MHz. From 6 and Table 5, we can observe that the numerical and analytical results are almost identical for different numbers of source nodes, demonstrating the accuracy of the analytical results. Additionally, the probability of interruption decreases with a higher latency threshold, as increasing the latency threshold improves the system's ability to meet the latency requirements. Furthermore, as the number of source nodes N increases, the outage probability decreases, indicating that multiple source nodes participating in offloading can effectively reduce the outage probability.

5. Conclusions

This paper presented a real-time distributed computing model that addressed low-voltage flow data in digital power grids operating in autonomous and controllable environments. The proposed model utilized edge computing through wireless offloading to process and analyze the data generated by low-voltage devices more efficiently. Firstly, we evaluated the performance of the system under consideration by measuring its outage probability, utilizing both the received signal-to-noise ratio (SNR) and communication and computing latency. Subsequently, we analyzed the system outage probability by deriving an analytical expression. To this end, we utilized the Gauss-Chebyshev approximation to provide an approximate closed-form expression. Experimental evaluations indicated that the proposed model effectively achieved real-time processing of low-voltage flow data in digital power grids. This model offered an effective and practical solution for handling low-voltage flow data, making it a valuable addition to the digital power grids domain.

5.1. Copyright

6. Acknowledgements

The work in this paper was supported by the Innovation Project of China Southern Power Grid (No. GDKJXM20210995).

References

[1] W. Hong, J. Yin, M. You, H. Wang, J. Cao, J. Li, and M. Liu, "Graph intelligence enhanced bi-channel insider threat detection," in *Network and System Security: 16th*

International Conference, NSS 2022, Denarau Island, Fiji, December 9–12, 2022, Proceedings. Springer, 2022, pp. 86–102.

[2] S. Guo and X. Zhao, "Multi-agent deep reinforcement learning based transmission latency minimization for delay-sensitive cognitive satellite-uav networks," *IEEE Trans. Commun.*, vol. 71, no. 1, pp. 131–144, 2023.

[3] Y. Wu and C. Gao, "Intelligent resource allocation scheme for cloud-edge-end framework aided multi-source data stream," *to appear in EURASIP J. Adv. Signal Process.*, vol. 2023, no. 1, 2023.

[4] K. Li and J. C. Príncipe, "Functional bayesian filter," *IEEE Trans. Signal Process.*, vol. 70, pp. 57–71, 2022.

[5] J. Yin, M. Tang, J. Cao, M. You, H. Wang, and M. Alazab, "Knowledge-driven cybersecurity intelligence: software vulnerability co-exploitation behaviour discovery," *IEEE Transactions on Industrial Informatics*, 2022.

[6] H. Wan and A. Nosratinia, "Short-block length polar-coded modulation for the relay channel," *IEEE Trans. Commun.*, vol. 71, no. 1, pp. 26–39, 2023.

[7] X. Zheng and C. Gao, "Intelligent computing for WPT-MEC aided multi-source data stream," *to appear in EURASIP J. Adv. Signal Process.*, vol. 2023, no. 1, 2023.

[8] Z. Xie, W. Chen, and H. V. Poor, "A unified framework for pushing in two-tier heterogeneous networks with mmwave hotspots," *IEEE Trans. Wirel. Commun.*, vol. 22, no. 1, pp. 19–31, 2023.

[9] J. Yin, M. Tang, J. Cao, H. Wang, M. You, and Y. Lin, "Vulnerability exploitation time prediction: an integrated framework for dynamic imbalanced learning," *World Wide Web*, pp. 1–23, 2022.

[10] B. Han, V. Sciancalepore, Y. Xu, D. Feng, and H. D. Schotten, "Impatient queuing for intelligent task offloading in multiaccess edge computing," *IEEE Trans. Wirel. Commun.*, vol. 22, no. 1, pp. 59–72, 2023.

[11] R. Zhao and M. Tang, "Profit maximization in cache-aided intelligent computing networks," *Physical Communication*, vol. PP, no. 99, pp. 1–10, 2022.

[12] R. Zhang, B. Shim, and W. Wu, "Direction-of-arrival estimation for large antenna arrays with hybrid analog and digital architectures," *IEEE Trans. Signal Process.*, vol. 70, pp. 72–88, 2022.

[13] W. Zhou and F. Zhou, "Profit maximization for cache-enabled vehicular mobile edge computing networks," *IEEE Trans. Vehic. Tech.*, vol. PP, no. 99, pp. 1–6, 2023.

[14] L. Chen and X. Lei, "Relay-assisted federated edge learning:Performance analysis and system optimization," *IEEE Transactions on Communications*, vol. PP, no. 99, pp. 1–12, 2022.

[15] M. Zaher, Ö. T. Demir, E. Björnson, and M. Petrova, "Learning-based downlink power allocation in cell-free massive MIMO systems," *IEEE Trans. Wirel. Commun.*, vol. 22, no. 1, pp. 174–188, 2023.

[16] W. Zhou, L. Fan, F. Zhou, F. Li, X. Lei, W. Xu, and A. Nallanathan, "Priority-aware resource scheduling for UAV-mounted mobile edge computing networks," *IEEE Transactions on Vehicular Technology*, 2023.

[17] R. Yang, Z. Zhang, X. Zhang, C. Li, Y. Huang, and L. Yang, "Meta-learning for beam prediction in a dual-band communication system," *IEEE Trans. Commun.*, vol. 71, no. 1, pp. 145–157, 2023.

[18] J. Ling and C. Gao, "DQN based resource allocation for NOMA-MEC aided multi-source data stream," *to appear in EURASIP J. Adv. Signal Process.*, vol. 2023, no. 1, 2023.

[19] P. Hoher, S. Wirtensohn, T. Baur, J. Reuter, F. Govaers, and W. Koch, "Extended target tracking with a lidar sensor using random matrices and a virtual measurement model," *IEEE Trans. Signal Process.*, vol. 70, pp. 228–239, 2022.

[20] S. Tang and L. Chen, "Computational intelligence and deep learning for next-generation edge-enabled industrial IoT," *IEEE Trans. Netw. Sci. Eng.*, vol. 9, no. 3, pp. 105–117, 2022.

[21] B. Banerjee, R. C. Elliott, W. A. Krzymien, and H. Farmanbar, "Downlink channel estimation for FDD massive MIMO using conditional generative adversarial networks," *IEEE Trans. Wirel. Commun.*, vol. 22, no. 1, pp. 122–137, 2023.

[22] L. He and X. Tang, "Learning-based MIMO detection with dynamic spatial modulation," *IEEE Transactions on Cognitive Communications and Networking*, vol. PP, no. 99, pp. 1–12, 2023.

[23] J. Chen, X. Cao, P. Yang, M. Xiao, S. Ren, Z. Zhao, and D. O. Wu, "Deep reinforcement learning based resource allocation in multi-uav-aided MEC networks," *IEEE Trans. Commun.*, vol. 71, no. 1, pp. 296–309, 2023.

[24] L. Zhang and S. Tang, "Scoring aided federated learning on long-tailed data for wireless iomt based healthcare system," *IEEE Journal of Biomedical and Health Informatics*, vol. PP, no. 99, pp. 1–12, 2023.

[25] D. Orlando, S. Bartoletti, I. Palamà, G. Bianchi, and N. Blefari-Melazzi, "Innovative attack detection solutions for wireless networks with application to location security," *IEEE Trans. Wirel. Commun.*, vol. 22, no. 1, pp. 205–219, 2023.

[26] R. Zhao, C. Fan, J. Ou, D. Fan, J. Ou, and M. Tang, "Impact of direct links on intelligent reflect surface-aided mec networks," *Physical Communication*, vol. 55, p. 101905, 2022.

[27] M. E. Gonzalez, J. F. Silva, M. Videla, and M. E. Orchard, "Data-driven representations for testing independence: Modeling, analysis and connection with mutual information estimation," *IEEE Trans. Signal Process.*, vol. 70, pp. 158–173, 2022.

[28] S. Tang and X. Lei, "Collaborative cache-aided relaying networks: Performance evaluation and system optimization," *IEEE Journal on Selected Areas in Communications*, vol. 41, no. 3, pp. 706–719, 2023.